

Dynamics of the molecular geometric phase

Rocco Martinazzo^{1,2,*}, Irene Burghardt³

¹*Department of Chemistry, Università degli Studi di Milano, Via Golgi 19, 20133 Milano, Italy**

²*Istituto di Scienze e Tecnologie Molecolari, CNR, via Golgi 19, 20133 Milano, Italy and*

³*Institute of Physical and Theoretical Chemistry, Goethe University Frankfurt, Max-von-Laue-Str. 7, D-60438 Frankfurt/Main, Germany*

The fate of the molecular geometric phase in an exact dynamical framework is investigated with the help of the exact factorization of the wavefunction and a recently proposed quantum hydrodynamical description of its dynamics. An instantaneous, gauge invariant phase is introduced for arbitrary paths in nuclear configuration space in terms of hydrodynamical variables, and shown to reduce to the adiabatic geometric phase when the state is adiabatic and the path is closed. The evolution of the closed-path phase over time is shown to adhere to a Maxwell-Faraday induction law, with non-conservative forces arising from the electron dynamics that play the role of electromotive forces. We identify the pivotal forces that are able to change the value of the phase, thereby challenging any topological argument. Nonetheless, negligible changes in the phase occur when the local dynamics along the probe loop is approximately adiabatic. In other words, the adiabatic idealization of geometric phase effects may remain suitable for effectively describing certain dynamic observables.

Introduction. Geometric phases are fundamental concepts in physics and chemistry, with wide-ranging implications. They are closely associated with various phenomena, such as the quantum, the anomalous and the spin Hall effect [1, 2], the exotic physics of topological insulators [3, 4], dielectric polarization in crystals [2, 5–9], the Aharonov-Bohm effect [10], and conical intersections (CIs) in molecules [11–13]. Geometric phases usually emerge when the Hamiltonian of a system depends on a set of “environmental” parameters \mathbf{x} which, in Berry’s original work [14], are allowed to change adiabatically, but they remain well defined concepts for non-adiabatic, non-cyclic and non-unitary evolutions as well [15–18]. In the case of molecules, geometric phases play a critical role around an intersection between two or more potential energy surfaces. Even when the molecular dynamics remains nearly adiabatic, the presence of a CI can significantly impact the outcome of a chemical reaction [19–21], because of the quantum interference of wavepackets encircling the CI that crucially depends on the geometric phase [22, 23]. In these molecular problems, the Berry phase is often not just geometric but also topological, that is, it is independent of both the dynamics and the path (as long as homotopic paths are compared). In fact, it is the phase introduced as early as 1958 by Longuet-Higgins [24, 25] that is known to control the energy level ordering in, e.g., Jahn-Teller systems. However, these intriguing properties depend crucially on the adiabatic description (approximation) of the dynamics, and it is uncertain whether and how they persist when the *exact* quantum dynamics is considered. Recent works [26, 27] have shown that the topological character of the phase is an artifact of the adiabatic approximation and suggest, more generally, that the geometric phase in molecules may be a less useful concept than previously believed.

The purpose of this work is to shed light on these issues and to reconcile the adiabatic perspective with the exact dynamical evolution. To this end we will first show that a geometric phase is yet meaningful when the full electron-nuclear system is in a pure state. We will use the framework of the exact factorization (EF) of the molecular wavefunction [28, 29] since this construction extends the fiber structure of the adiabatic approximation to arbitrary states, thereby enabling a natural extension of the Berry phase [30]. Subsequently, we will explore the exact dynamical evolution of this phase. This task is challenging when using the original equations of motion of the EF approach due to their inherent *gauge* freedom. However, a recently developed quantum hydrodynamical (QHD) description of the EF dynamics [31] makes this step feasible. QHD offers an alternative formulation for electron-nuclear dynamics, relying on EF while employing only *gauge*-invariant variables [31]. Within this QHD-EF framework we will identify the key factors influencing the evolution of the geometric phase and analyze a model two-state problem.

Gauge invariant EF dynamics. In the exact factorization approach [28, 29] the wavefunction is represented exactly as

$$|\Psi\rangle = \int_{\mathbf{x}} d\mathbf{x} \psi(\mathbf{x}) |u(\mathbf{x})\rangle |\mathbf{x}\rangle \quad (1)$$

where $\{|\mathbf{x}\rangle\}$ is the position basis of the nuclear variables x^k ($k = 1, 2, \dots, N$), $|u(\mathbf{x})\rangle$ is the conditional electronic state at \mathbf{x} and $\psi(\mathbf{x})$ is the marginal probability amplitude for the nuclei, i.e. the “nuclear wavefunction”. The latter two can be obtained, up to a *gauge* choice, by projecting the total wavefunction on the nuclear basis states and imposing a normalization condition on the ensuing local electronic states,

$$\langle \mathbf{x} | \Psi \rangle_X = \psi(\mathbf{x}) |u(\mathbf{x})\rangle \equiv |\Psi(\mathbf{x})\rangle \langle u(\mathbf{x}) | u(\mathbf{x}) \rangle = 1 \quad (2)$$

where the subscript X indicates that integration is performed over nuclear variables only. In the EF approach

* rocco.martinazzo@unimi.it

$\psi(\mathbf{x})$ and $|u(\mathbf{x})\rangle$ evolve in time according to equations of motion that can be derived from either the variational principle or projection operator techniques, as shown, respectively, in Refs. [28, 29] or Refs. [32, 33]. In the QHD description of the dynamics [31] the nuclear wavefunction is replaced by a probability fluid with density $n(\mathbf{x}) = |\psi(\mathbf{x})|^2$ and velocity field $v^k(\mathbf{x})$, and the electronic state is described by electronic density operators $\rho_{\text{el}}(\mathbf{x}) = |u(\mathbf{x})\rangle\langle u(\mathbf{x})|$ tied to the fluid elements. The equations of motion consist of a continuity equation for the density, $\partial_t n + \sum_k \partial_k (n v^k) = 0$, a momentum equation

$$\dot{\pi}_k = -\text{Tr}_{\text{el}}(\rho_{\text{el}} \partial_k H_{\text{el}}) - \frac{\hbar^2}{n} \sum_{ij} \xi^{ij} \partial_i (n g_{kj}) - \partial_k Q \quad (3)$$

and a Liouville-von Neumann-like equation for the conditional electronic density operators,

$$i\hbar \dot{\rho}_{\text{el}} = [H_{\text{el}} + \delta H_{\text{en}}, \rho_{\text{el}}] \quad (4)$$

In the above equations the dot denotes the material (i.e., Lagrangian) derivative, $\dot{f} \equiv \partial_t f + \sum_k v^k \partial_k f$, ξ^{ij} is the inverse mass tensor of the nuclear system, $Q = -\hbar^2/2 \sum_{ij} \xi^{ij} n^{-1/2} \partial_i \partial_j n^{1/2}$ is the Bohm quantum potential [34], $H_{\text{el}} = H_{\text{el}}(\mathbf{x})$ is the local electronic Hamiltonian and δH_{en} is the electron-nuclear coupling

$$\delta H_{\text{en}} = -\frac{\hbar^2}{2n} \sum_{ij} \xi^{ij} \partial_i (n \partial_j \rho_{\text{el}}) \quad (5)$$

Furthermore, g_{kj} is the Fubini-Study (FS) metric [35], which is the real part of the quantum geometric tensor [14]

$$q_{kj} = \text{Tr}_{\text{el}}(\rho_{\text{el}} \partial_k \rho_{\text{el}} \partial_j \rho_{\text{el}}) \quad (6)$$

here expressed in terms of conditional density operators. The momentum field π_k is related to the velocity field through the inverse mass tensor, $v^k = \sum_j \xi^{kj} \pi_j$, and is connected to the EF wavefunction by $\pi_k = \Re(\hat{p}_k \psi / \psi) - \hbar A_k$, where $\hat{p}_k = -i\hbar \partial_k$ is the canonical momentum operator and A_k is the Berry connection, $A_k = i \langle u | \partial_k u \rangle$. It can also be obtained from the total electronic-nuclear ($e-n$) wavefunction, without referring to the EF, since $\pi_k \equiv n^{-1}(\mathbf{x}) \Re \langle \Psi(\mathbf{x}) | \hat{p}_k | \Psi(\mathbf{x}) \rangle_{\text{el}}$, where $|\Psi(\mathbf{x})\rangle$ was introduced in Eq. 2 and the subscript el means that integration is performed over electronic variables only. The circulation of π_k around arbitrary closed paths γ in nuclear configuration space satisfies a quantization condition

$$\sum_k \oint_{\gamma} (\pi_k + \hbar A_k) dx^k = 2\pi \hbar n \quad n \in \mathbb{Z} \quad (7)$$

which merely expresses the fact that the nuclear wavefunction ψ must be smooth around any loop. Here, n is the topological value that describes the way the wavefunction phase winds around a singularity of the momentum field (for instance, a wavefunction node). In fact, n can be nonzero only in a multiply connected domain,

when γ cannot be shrunk to a single point. The condition of Eq. 7 needs to be imposed at the initial time only (with a smooth choice of the phases of the nuclear and electronic wavefunctions in Eq. 2), since Kelvin's circulation theorem holds for the fluid dynamics described here [31]. Hence, in principle, the EF nuclear and electronic wavefunctions are needed only at the initial time, and n , π_k and ρ_{el} can then be obtained at any time upon solving the above *gauge*-invariant equations of motion, i.e., Eqs. 3, 4 jointly with the continuity equation. In the following we shall focus on a given instant of time and investigate the geometric properties of the instantaneous fiber bundle induced by the EF of the total wavefunction.

Non-adiabatic geometric phase. The quantization condition of Eq. 7 shows that the momentum field π_k can be used to define a *gauge* invariant, instantaneous "phase" for arbitrary paths γ in configuration space

$$\Gamma[\gamma] = -\frac{1}{\hbar} \sum_k \int_{\gamma} \pi_k dx^k \quad (8)$$

For closed paths this reduces, by construction, to the holonomy of the vector bundle defined by the EF representation of the wavefunction (see Eq. 7)

$$\Gamma_{\text{el}}[\gamma] = \sum_k \oint_{\gamma} A_k dx^k \pmod{2\pi} \quad (9)$$

and, more generally, it defines a quantity which is *gauge* invariant even when the path is open. In fact, for a curve γ that connects \mathbf{x}_a to \mathbf{x}_b , $\Gamma[\gamma]$ is the sum of two contributions that are separately invariant,

$$\Gamma[\gamma] = -\Theta_{ba} + \Gamma_{\text{el}}[\gamma] \quad (10)$$

where $\Theta_{ba} = \arg \langle \Psi(\mathbf{x}_a) | \Psi(\mathbf{x}_b) \rangle$ and $\Gamma_{\text{el}}[\gamma]$ is a purely electronic term

$$\Gamma_{\text{el}}[\gamma] = \arg \langle u(\mathbf{x}_a) | u(\mathbf{x}_b) \rangle + \sum_k \int_{\gamma} A_k dx^k \quad (11)$$

The first term, Θ_{ba} , is the Pancharatnam phase difference (valid for arbitrary non-orthogonal vectors) of the total electron-nuclear wavefunction between b and a , while the second term, $\Gamma_{\text{el}}[\gamma]$ is the Pancharatnam phase accumulated by the electronic vector when parallel transported from \mathbf{x}_a to \mathbf{x}_b along γ [15, 17, 18, 36, 37][38]. Indeed, $\pi_k \equiv \hbar \partial_k \theta - \hbar A_k$ (where $\theta = \arg \psi$) and the phase change of the nuclear wavefunction at the endpoints of the curve, $\Delta \theta = \theta_b - \theta_a$, can be written as $\Delta \theta = \arg(\psi_a^* \psi_b \langle u_a | u_b \rangle) - \arg(\langle u_a | u_b \rangle)$, where $\psi(\mathbf{x}) |u(\mathbf{x})\rangle = |\Psi(\mathbf{x})\rangle$. In a sense, $-\Gamma[\gamma]$ is a *nuclear* phase, i.e., the phase difference of the total wavefunction minus that of the electronic one. That is, $\Theta_{ba} = -\Gamma[\gamma] + \Gamma_{\text{el}}[\gamma]$ is a decomposition of the total phase difference into nuclear and electronic contributions. For a loop $\Theta_{ba} \equiv 0$ and the nuclear phase difference is the opposite of the electronic one, which in this case reduces to Eq. 9.

Importantly, $\Gamma[\gamma]$ is only indirectly tied to the connection defined by the EF: it is a property that relies

on EF but does not require that the EF of the wavefunction is performed. Its definition is further consistent with the fluid dynamics: for stationary loops the quantization condition (Eq. 7) jumps eventually by $\pm 2\pi$ during the dynamics (every time a wavefunction node crosses the loop [31]) but this does not affect the above identities.

Dynamics. We now focus on the phase defined by Eq. 8, evaluated for a path γ that is a loop, fixed in time, and use the symbol $\Gamma_O[\gamma]$ to emphasize that the path is closed. The dynamical evolution of $\Gamma_O[\gamma]$ is determined by the momentum equation, upon observing that $\partial_t \pi_k = \dot{\pi}_k - \sum_j v^j \partial_j \pi_k$. Here, the first term is the force acting on the fluid elements (Eq. 3) and the second one (the advective contribution) can be rearranged as $\sum_j v^j \partial_j \pi_k = \sum_j v^j \partial_k \pi_j + \sum_j v^j B_{kj}$, where only the second term contributes to $\Gamma_O[\gamma]$, since the first one is the k^{th} derivative of the classical kinetic energy $T = \sum_{ij} \xi^{ij} \pi_i \pi_j$. Furthermore, B_{kj} is the kj component of the curvature tensor $B_{kj} = \hbar(\partial_k A_j - \partial_j A_k) = -2\hbar \Im q_{kj}$, with the result that the rate of change of the phase displays three distinct, *gauge*-invariant contributions,

$$-\frac{d\Gamma_O[\gamma]}{dt} = \mathfrak{E}^{\text{NBO}} + \mathfrak{E}^{\text{el}} + \mathfrak{E}^{\text{mag}} \quad (12)$$

Here,

$$\mathfrak{E}^{\text{NBO}} = -\frac{1}{\hbar} \oint_{\gamma} \sum_k \text{Tr}_{\text{el}}(\rho_{\text{el}} \partial_k H_{\text{el}}) dx^k \quad (13)$$

is a non-adiabatic contribution driven by the electronic Hamiltonian, and

$$\mathfrak{E}^{\text{el}} = -\hbar \oint_{\gamma} \sum_{ijk} \frac{\xi^{ij}}{n} \partial_i (n g_{kj}) dx^k \quad (14)$$

$$\mathfrak{E}^{\text{mag}} = -\frac{1}{\hbar} \oint_{\gamma} \sum_{jk} v^j B_{kj} dx^k \quad (15)$$

are geometric contributions related, respectively, to the *pseudo*-electric and *pseudo*-magnetic *gauge* fields acting on the nuclei.

Eq. 13 represents a genuine non-Born-Oppenheimer contribution entirely due to the non-conservative part of the Ehrenfest force $F_k^{\text{Eh}} = -\text{Tr}_{\text{el}}(\rho_{\text{el}} \partial_k H_{\text{el}})$ appearing in Eq. 3. It is tied to the non-stationarity of the local electronic states since it disappears when the system is in an adiabatic state, i.e. when setting $|u(\mathbf{x})\rangle$ to be eigenstate of the local electronic Hamiltonian $H_{\text{el}}(\mathbf{x})$. The second contribution, Eq. 14, is generally non-vanishing, and it depends on the (instantaneous) electronic state through the metric properties of the EF fiber bundle (the FS metric g_{kj}) and on the nuclear state through the density n . The third contribution, Eq. 15, on the other hand, is (possibly) non-vanishing only when the nuclear state is current-carrying. It appears here only because we fixed the loop: the phase is tied to the local electronic states

that, in turn, move in tandem with the fluid elements describing the nuclear probability density. In other words, if we allowed the loop to follow the fluid dynamics we would find

$$-\frac{d\tilde{\Gamma}_O[\gamma]}{dt} = \mathfrak{E}^{\text{NBO}} + \mathfrak{E}^{\text{el}} \quad (16)$$

where now $\tilde{\Gamma}_O[\gamma]$ refers to the geometric phase along a loop γ that follows the fluid flow (see SM).

The above findings are general, and hold for arbitrary electronic-nuclear states. For cases where Stokes's theorem applies they can be anticipated by the Maxwell-Faraday induction law

$$-\partial_t \mathcal{B} = d\mathcal{E} \quad (17)$$

that holds for the *gauge* fields governing the nuclear dynamics in the EF approach [31]. Here, d denotes the exterior derivative, $\mathcal{B} = d\omega$ is the Berry curvature 2-form, $\omega = \hbar \sum_k A_k dx^k$ is the 1-form associated with the Berry connection, and $\mathcal{E} = i\hbar d \langle u | \partial_t u \rangle - \partial_t \omega = \sum_k E_k dx^k$ is the *gauge*-invariant 1-form defining the *pseudo*-electric field E_k [39]. Indeed, application of Stokes' theorem to an open surface having γ as a boundary, and identification of the *pseudo*-electric field E_k acting on the nuclei (see Section III.A of Ref. [31] and, in particular, Eq. 59) leads again to Eqs. 12-15. Compared to the Maxwell-Faraday induction law of classical electromagnetism, though, here there is no varying magnetic flux inducing an electromotive force on a circuit. Rather, it is the magnetic flux (i.e. the geometric phase) of the electronic subsystem that changes *because* of the non-conservative work done by the electrons on the nuclei, around the loop γ in nuclear configuration space. That is, Eq. 17 becomes a reversed-induction law.

Of main interest here is the analysis of the adiabatic geometric phase, i.e. the rate of phase change defined by Eq. 12 when the system is found in an adiabatic state and, in particular, when the phase is topological. In this situation, as mentioned above, the non-Born-Oppenheimer circulation of Eq. 13 vanishes since the Ehrenfest force becomes conservative. However, also the "drift", *pseudo*-magnetic term of Eq. 15 disappears since $\mathcal{B} \equiv 0$ (almost everywhere) if the phase is topological. Hence, we are left with the *pseudo*-electric work of Eq. 14 which thus represents the key factor affecting a phase which is found topological in the adiabatic approximation, at least at short time when departing from the adiabatic state. Since Eq. 14 is generally non-zero and path-dependent, the phase which is topological in the adiabatic state becomes geometric. Indeed, the curvature departs from zero according to the induction law, Eq. 17, driven by the local vorticity of the *pseudo*-electric field which is generally non-zero. Hence, \mathcal{B} becomes non-zero and the phase cannot remain topological. In the following we address a model two-state problem that exemplifies the transition between topological and geometric phase.

Model two-state problem. We now consider a 2-state model that highlights the key features of a molecu-

lar problem involving a CI. The nuclear system contains a number of degrees of freedom described by $\mathbf{x} \in \mathcal{M} \cong \mathbb{R}^N$ and the electronic Hamiltonian takes the general form (in a diabatic basis [40]) $H_{\text{el}} = A(\mathbf{x})\sigma_0 + \mathbf{B}(\mathbf{x})\boldsymbol{\sigma}$, where $A(\mathbf{x})$ is a scalar, $\mathbf{B}(\mathbf{x}) \in \mathcal{N} \cong \mathbb{R}^3$ is an effective magnetic field, $\sigma_0 = \mathbb{I}_2$ is the 2x2 unit matrix and $\boldsymbol{\sigma} = (\sigma_x, \sigma_y, \sigma_z)$ is the vector of Pauli matrices.

The geometric properties of the adiabatic bundles are well-known [14, 41] and can be ‘‘pulled back’’ from the problem of a spin in a slowly varying magnetic field, with \mathcal{N} as parameter space [42]. Briefly, the Berry phase along a path $\gamma \subset \mathcal{M}$ is generally path-dependent and is given by $q_{\pm} = \mp \hbar/2$ times the solid angle subtended by the curve image $\tilde{\gamma} = \beta \circ \gamma$ generated in \mathcal{N} space by the magnetic field function, $\beta : \mathbf{x} \rightarrow \mathbf{B}(\mathbf{x})$. This is the flux of the ‘‘Berry field’’ $\mathbf{H}^{\pm} = q_{\pm} \mathbf{B}/B^3$ through an arbitrary surface subtending the curve $\tilde{\gamma}$ [43]. In a typical molecular problem, however, one of the \mathbf{B} components identically vanishes because of time-reversal symmetry, say B_z . Hence, the curvature in nuclear configuration space becomes $\mathcal{B}_{\pm} = H_z^{\pm} dB^x \wedge dB^y$ and it vanishes everywhere except at the CI seam. The image paths $\tilde{\gamma}$ necessarily lie in the xy plane of the \mathcal{N} space and the Berry phase becomes $\mp n\pi$, where n is the winding number of $\tilde{\gamma}$ around the origin of \mathcal{N} .

In the adiabatic approximation the magnetic field \mathbf{B} fully characterizes the electron dynamics (i.e., the energetics of the electronic problem) and the structure of the relevant bundle. For arbitrary electron-nuclear states (and an exact dynamics) we further need the polarization vector $\mathbf{s}(\mathbf{x}) \in \mathcal{N}$ that characterizes the conditional density matrix, $\rho_{\text{el}}(\mathbf{x}) = \frac{1}{2}(\sigma_0 + \mathbf{s}(\mathbf{x})\boldsymbol{\sigma})$ ($\|\mathbf{s}\| = 1$ for a pure state). Eq. 4 gives its dynamical equation in the form

$$\dot{\mathbf{s}} = (\Omega \mathbf{b} + \boldsymbol{\tau}) \times \mathbf{s} - \frac{\hbar}{2} \sum_{ij} \xi^{ij} \partial_i (\mathbf{s}_j \times \mathbf{s}) \quad (18)$$

where $\Omega = 2B/\hbar$ is the Larmor precession frequency, \mathbf{b} is the unit vector identifying the magnetic field direction, $\mathbf{s}_j := \partial_j \mathbf{s}$ and $\boldsymbol{\tau} = \sum_j u^j \mathbf{s}_j$ is the ‘‘nuclear torque’’, an effective field due to the e - n coupling that involves the osmotic velocity [44] $u^j = -\hbar/2 \sum_k \xi^{jk} \partial_k \ln n$. The bundle structure, on the other hand, is characterized by the quantum geometric tensor

$$q_{kj} = \frac{1}{4} (\mathbf{s}_k \mathbf{s}_j + i \mathbf{s}(\mathbf{s}_k \times \mathbf{s}_j)) \quad (19)$$

which gives $g_{kj} = \mathbf{s}_k \mathbf{s}_j / 4$ and $B_{kj} = -\hbar \mathbf{s}(\mathbf{s}_k \times \mathbf{s}_j) / 2$ (see SM). We can therefore express the contributions to the rate of phase change appearing on the r.h.s. of Eq. 12 as integrals of simple 1-forms, i.e. $\mathbf{e}^X = \oint_{\gamma} \Phi^X$ (for $X = \text{NBO, el and mag}$), where $\Phi^{\text{NBO}} = \hbar^{-1} \mathbf{B} ds$, $\Phi^{\text{el}} = 1/2 \boldsymbol{\tau} ds - \hbar/4 \sum_{ij} \xi^{ij} \partial_i \mathbf{s}_j ds$ and $\Phi^{\text{mag}} = 1/2 (\boldsymbol{\nu} \times \mathbf{s}) ds$, upon defining $\boldsymbol{\nu} = \sum_j v^j \mathbf{s}_j$. The circulations are therefore all mapped on the Bloch sphere $S^2 \subset \mathcal{N}$ (the projective Hilbert space of the 2-level system), where $\mathbf{s}(\mathbf{x})$ traces a curve $\tilde{\gamma}$ when \mathbf{x} moves along the curve γ . Note

that $\boldsymbol{\tau}, \boldsymbol{\nu}$ and ds are tangent to the sphere, while \mathbf{B} can have both tangent and normal components, depending on the real-space position \mathbf{x} . The results for an adiabatic state follow upon setting $\mathbf{s} = \pm \mathbf{b}$ for the upper and lower adiabatic states, respectively. In this case, as anticipated above, $\Phi^{\text{NBO}} = 0$ since \mathbf{b} is normal to S^2 . Furthermore, if the Berry phase is topological, $\boldsymbol{\nu}$ and ds are always parallel to each other, and we have $\Phi^{\text{mag}} = 0$, as seen above.

For concreteness, we consider 2+1 nuclear degrees of freedom ($\mathcal{M} \cong \mathbb{R}^3$) mimicking a one-dimensional CI seam, with parameter values typical of a molecular problem and a diagonal mass tensor, $\xi^{ij} = \delta^{ij} M^{-1}$, with $M = 1$ u.m.a.. Upon taking $A(\mathbf{x})$ independent of z the problem becomes effectively two-dimensional. Specifically, setting $A(\mathbf{x}) = \frac{1}{2} M \omega_x^2 x^2 + \frac{1}{2} M \omega_y^2 y^2$ ($\omega_x = \omega_y = \omega = 1000 \text{ cm}^{-1}$) and employing a linear vibronic coupling $\mathbf{B} = \kappa_x x \mathbf{e}_1 + \kappa_y y \mathbf{e}_2$ ($\kappa_x = \kappa_y = \kappa = 0.1$ a.u.) the problem becomes a standard, linear $E \otimes e$ Jahn-Teller model, with adiabatic states $E_{\pm}(\rho) = \frac{1}{2} M \omega^2 \rho^2 \pm \kappa \rho$ (Fig. 1), where ρ is the distance from the z axis. We solved the time-dependent Schrödinger equation for this problem using a standard Split-Operator algorithm in conjunction with Fast-Fourier-Transforms to go back and forth between real- and momentum-space. The wavefunction was represented on a fine grid (1024×1024), which was centered around the CI point and taken of length $20 a_0$ along each direction. A small time step of $\Delta t = 0.1$ a.u. was adopted to ensure a good sampling of the geometric phase over time. The initial wavefunction was obtained by combining a nuclear wavepacket $\psi_0(\mathbf{x})$ with a ground electronic state $|u_-(\mathbf{x})\rangle$, i.e. $\langle \mathbf{x} | \Psi_0 \rangle_X = \psi_0(\mathbf{x}) |u_-(\mathbf{x})\rangle$. The nuclear wavepacket $\psi_0(\mathbf{x})$ was a Gaussian centered at $x_0 = -2\kappa/M\omega^2$ and $y_0 = 0$, with ground-state width along both x and y ($\Delta x = \Delta y = \sqrt{\hbar/2m\omega}$) and zero nominal momentum along both directions. As for the electronic state, we fixed the *gauge* with the choice $|u_-(\mathbf{x})\rangle = (-e^{-i\phi} |1\rangle + |2\rangle) / \sqrt{2}$ where ϕ is the azimuthal angle of the position vector \mathbf{x} . With these choices the initial wavefunction is current-carrying, and presents a non-vanishing velocity field directed along the negative ϕ direction, albeit very small (with the chosen parameters) in the region where the wavepacket moves. A different choice of initial state is described in the SM, which also provides details about the two-state model, the numerical implementation of the dynamics and the calculation of the geometric phase. The latter was performed at every time step along a number of paths fixed in time, that were discretized on the numerical grid.

Fig. 1 shows the main results of our numerical investigation. The wavepacket spreads along the valley of the ‘‘Mexican hat’’ potential and its trailing edges meet each other and interfere at time $t \approx 75 fs$, after which the wavepacket covers more or less uniformly the valley, with a time-varying interference pattern (panels (b)-(d)). Fig. 1 (e) shows the evolution of the geometric phase (in π units) along three significant paths, i.e., three circles of radius $R = 2.0, 2.5$ and $3.0 a_0$ centered at the CI point.

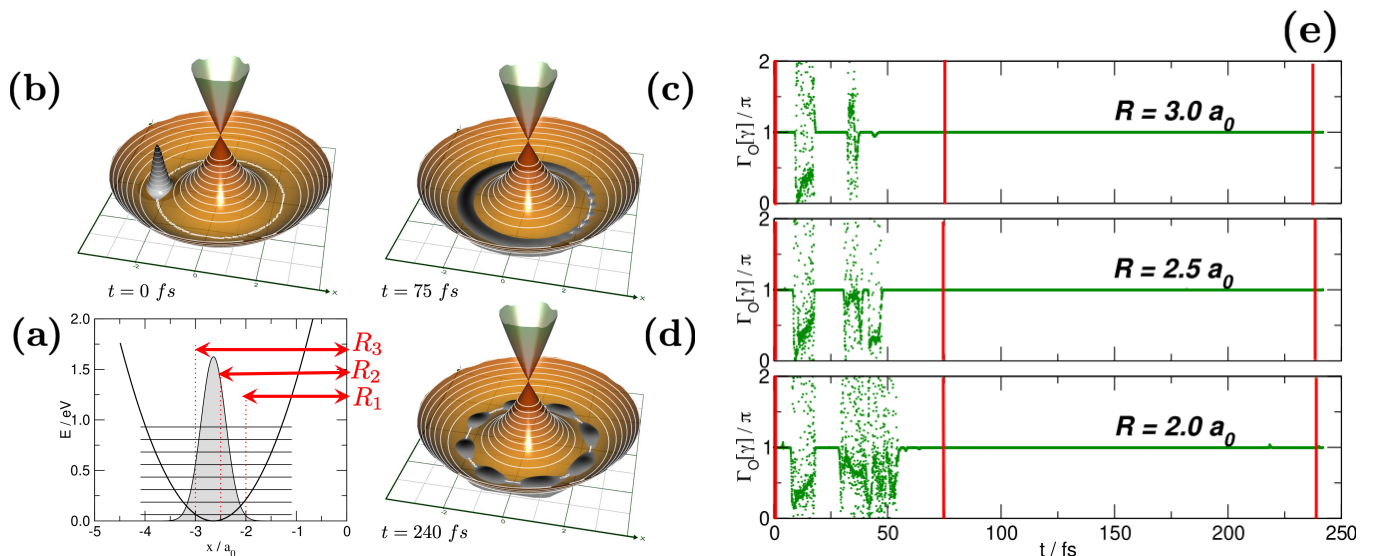


Figure 1. Exact quantum dynamical results for the two-dimensional, two-state model problem described in the main text, as obtained from a true adiabatic ground state at initial time. (a) Nuclear density at $t = 0$ along the x coordinate. Also shown the adiabatic ground-state potential and the ladder of vibrational states of the diabatic potential. The arrows denote the radii of some circular paths, centered at the CI point, along which the geometric phase was computed. (b)-(d) Snapshots of the nuclear density at three significant times, $t = 0, 75$ and 240 fs, as indicated. Also shown the adiabatic potential energy surfaces intersecting at the origin of the coordinate system. (e) Evolution of the geometric phase of Eq. 8 (in units of π) along the three paths marked in (a), namely for circles of radius $R = 2.0, 2.5$ and $3.0 a_0$ (from bottom to top, as indicated). The red vertical bars denote the three times chosen for panels (b)-(d). See text for details.

The behaviour of the phase at short time ($t \lesssim 20$ fs) is somewhat uncertain because of the intrinsic limits of the numerical implementation: the paths go through regions in space where the nuclear density is very small and the polarization field, as well as the momentum and velocity fields, get affected by sizable numerical errors (see SM for a discussion on this point and our fix). This problem, however, has no physical implications since the geometric phase is of little practical utility when the probe path along which the phase is computed lies entirely (or partially) in a region where the system has little probability to be found. After this transient, the phase is seen to undergo an evident variation — which is numerically robust — when the wavepacket edges start to interfere, and later gets back to the value expected for an adiabatic dynamics (Fig. 1 (e)). This provides direct evidence for the transition between geometric and topological phase, from the vantage point of exact quantum dynamics. Analysis of the contributions to the electromotive force confirms that the NBO component contributes little to the phase change, while the *pseudo*-electric one plays the major role

(see SM).

In this example the dynamics remains adiabatic to a large extent, with the excited-state probability never exceeding 10^{-5} . Non-adiabatic behaviour appears as a transient, and it is more marked closer to the CI, in accordance with the stronger non-adiabatic coupling experienced by the wavepacket there. In this situation, the concept of adiabatic geometric phase remains highly relevant, when the phase itself is computed along physically meaningful paths.

Conclusions. We have shown that the molecular geometric phase of the adiabatic approximation can be seamlessly extended to exact quantum dynamics. The generalized phase is time dependent and its evolution is governed by a (reversed) Maxwell-Faraday induction law, with non-conservative forces arising from the electron dynamics that play the role of electromotive forces. Though generally evolving in a complicated way, this geometric phase remains highly relevant when the dynamics is close to adiabatic and a physically motivated choice of the path is performed.

-
- [1] S. M. Girvin and K. Yang, Modern Condensed Matter Physics, Modern Condensed Matter Physics [10.1017/9781316480649](https://doi.org/10.1017/9781316480649) (2019).
 [2] D. Vanderbilt, Berry Phases in Electronic Structure Theory: Electric Polarization, Orbital Magnetization and Topological Insulators, Berry Phases in Electronic Struc-

- ture Theory [10.1017/9781316662205](https://doi.org/10.1017/9781316662205) (2018).
 [3] M. Z. Hasan and C. L. Kane, Colloquium: Topological insulators, *Reviews of Modern Physics* **82**, 3045 (2010).
 [4] C. L. Kane, Topological Band Theory and the Z2 Invariant, *Contemporary Concepts of Condensed Matter Science* **6**, 3 (2013).

- [5] R. Resta, Theory of the electric polarization in crystals, *Ferroelectrics* **136**, 51 (1992).
- [6] R. D. King-Smith and D. Vanderbilt, Theory of polarization of crystalline solids, *Physical Review B* **47**, 1651 (1993).
- [7] R. Resta, Macroscopic polarization in crystalline dielectrics: the geometric phase approach, *Reviews of Modern Physics* **66**, 899 (1994).
- [8] R. Resta, Manifestations of Berry’s phase in molecules and condensed matter, *Journal of Physics: Condensed Matter* **12**, R107 (2000).
- [9] D. Xiao, M. C. Chang, and Q. Niu, Berry phase effects on electronic properties, *Reviews of Modern Physics* **82**, 1959 (2010), arXiv:0907.2021.
- [10] Y. Aharonov and D. Bohm, Significance of electromagnetic potentials in the quantum theory, *Physical Review* **115**, 485 (1959).
- [11] C. A. Mead, The geometric phase in molecular systems, *Reviews of Modern Physics* **64**, 51 (1992).
- [12] D. R. Yarkony, Diabolical conical intersections, *Reviews of Modern Physics* **68**, 985 (1996).
- [13] B. K. Kendrick, Geometric phase effects in chemical reaction dynamics and molecular spectra, *Journal of Physical Chemistry A* **107**, 6739 (2003).
- [14] M. Berry, Quantal phase factors accompanying adiabatic changes, *Proceedings of the Royal Society of London. A. Mathematical and Physical Sciences* **392**, 45 (1984).
- [15] B. Simon, Holonomy, the Quantum Adiabatic Theorem, and Berry’s Phase, *Physical Review Letters* **51**, 2167 (1983).
- [16] Y. Aharonov and J. Anandan, Phase change during a cyclic quantum evolution, *Physical Review Letters* **58**, 1593 (1987).
- [17] R. Simon and N. Mukunda, Bargmann invariant and the geometry of the Güoy effect, *Physical Review Letters* **70**, 880 (1993).
- [18] N. Mukunda and R. Simon, Quantum Kinematic Approach to the Geometric Phase. I. General Formalism, *Annals of Physics* **228**, 205 (1993).
- [19] J. C. Juanes-Marcos, S. C. Althorpe, and E. Wrede, Chemistry: Theoretical study of geometric phase effects in the hydrogen-exchange reaction, *Science* **309**, 1227 (2005).
- [20] D. Yuan, Y. Huang, W. Chen, H. Zhao, S. Yu, C. Luo, Y. Tan, S. Wang, X. Wang, Z. Sun, and X. Yang, Observation of the geometric phase effect in the $\text{H}+\text{HD}\rightarrow\text{H}_2+\text{D}$ reaction below the conical intersection, *Nature Communications* **2020** 11:1 **11**, 1 (2020).
- [21] B. K. Kendrick, J. Hazra, and N. Balakrishnan, The geometric phase controls ultracold chemistry, *Nature Communications* **2015** 6:1 **6**, 1 (2015).
- [22] S. C. Althorpe, General explanation of geometric phase effects in reactive systems: Unwinding the nuclear wave function using simple topology, *Journal of Chemical Physics* **124**, 10.1063/1.2161220/349125 (2006).
- [23] C. H. Valahu, V. C. Olaya-Agudelo, R. J. MacDonell, T. Navickas, A. D. Rao, M. J. Millican, J. B. Pérez-Sánchez, J. Yuen-Zhou, M. J. Biercuk, C. Hempel, T. R. Tan, and I. Kassal, Direct observation of geometric-phase interference in dynamics around a conical intersection, *Nature Chemistry* **2023** , 1 (2023).
- [24] H. C. Longuet-Higgins, U. Öpik, M. H. L. Pryce, and R. A. Sack, Studies of the Jahn-Teller effect .II. The dynamical problem, *Proceedings of the Royal Society of London. Series A. Mathematical and Physical Sciences* **244**, 1 (1958).
- [25] G. Herzberg and H. C. Longuet-Higgins, Intersection of potential energy surfaces in polyatomic molecules, *Discussions of the Faraday Society* **35**, 77 (1963).
- [26] S. K. Min, A. Abedi, K. S. Kim, and E. K. Gross, Is the molecular berry phase an artifact of the Born-Oppenheimer approximation?, *Physical Review Letters* **113**, 263004 (2014), arXiv:1402.0227.
- [27] R. Requist, F. Tandetzky, and E. K. Gross, Molecular geometric phase from the exact electron-nuclear factorization, *Physical Review A* **93**, 042108 (2016).
- [28] A. Abedi, N. T. Maitra, and E. K. U. Gross, Exact Factorization of the Time-Dependent Electron-Nuclear Wave Function, *Physical Review Letters* **105**, 123002 (2010).
- [29] A. Abedi, N. T. Maitra, and E. K. U. Gross, Correlated electron-nuclear dynamics: Exact factorization of the molecular wavefunction, *The Journal of Chemical Physics* **137**, 22A530 (2012).
- [30] Henceforth, we shall use the term Berry phase to mean the “adiabatic geometric phase”.
- [31] R. Martinazzo and I. Burghardt, Quantum hydrodynamics of coupled electron-nuclear systems, *arXiv preprint* , 2310.08766 (2023), arXiv:2310.08766.
- [32] R. Martinazzo and I. Burghardt, Quantum Dynamics with Electronic Friction, *Physical Review Letters* **128**, 206002 (2022), arXiv:2108.02622.
- [33] R. Martinazzo and I. Burghardt, Quantum theory of electronic friction, *Physical Review A* **105**, 052215 (2022).
- [34] P. R. Holland, The Quantum Theory of Motion: An Account of the de Broglie-Bohm Causal Interpretation of Quantum Mechanics, *The Quantum Theory of Motion* 10.1017/CBO9780511622687 (1993).
- [35] J. P. Provost and G. Vallee, Riemannian structure on manifolds of quantum states, *Communications in Mathematical Physics* **76**, 289 (1980).
- [36] A. K. Pati, New derivation of the geometric phase, *Physics Letters A* **202**, 40 (1995).
- [37] A. K. Pati, Adiabatic Berry Phase and Hannay Angle for Open Paths, *Annals of Physics* **270**, 178 (1998), arXiv:9804057 [quant-ph].
- [38] The underlying connection being, of course, the instantaneous Berry connection defined by the EF of the wavefunction.
- [39] There is some freedom in defining this field, since one can add any *gauge*-invariant closed form to \mathcal{E} without altering the induction law and its *gauge* invariance. For instance, one can choose to add conservative forces in the form $\mathcal{F} = d\mathcal{V}$, where \mathcal{V} is a (*gauge* invariant) scalar potential acting on the nuclei. The important, non conservative, part of \mathcal{E} is the electron dynamical force F_k^{ED} first introduced in Ref. [32]: in the adiabatic approximation $F_k^{\text{ED}} \equiv 0$ and the geometric phase is stationary.
- [40] H. Köuppel, W. Domcke, and L. S. Cederbaum, Multimode Molecular Dynamics Beyond the Born-Oppenheimer Approximation (John Wiley & Sons, Ltd, 1984) pp. 59–246.
- [41] A. Bohm, A. Mostafazadeh, H. Koizumi, Q. Niu, and J. Zwanziger, *The Geometric Phase in Quantum Systems* (Springer Berlin Heidelberg, 2003).
- [42] More precisely, the quantum geometric tensor q in parameter space \mathcal{M} is the pullback by the magnetic field $\beta : \mathcal{M} \rightarrow \mathcal{N}$ of the fundamental geometric tensor \tilde{q} in \mathcal{N} , i.e., $q_{\mathbf{x}}(\mathbf{u}, \mathbf{v}) = (\beta^* \tilde{q})_{\mathbf{x}}(\mathbf{u}, \mathbf{v}) \equiv \tilde{q}_{\beta(\mathbf{x})}(d\beta_{\mathbf{x}}(\mathbf{u}), d\beta_{\mathbf{x}}(\mathbf{v}))$ for

$\mathbf{x} \in \mathcal{M}$ and $\mathbf{u}, \mathbf{v} \in T_{\mathbf{x}}\mathcal{M}$. Here $\beta : \mathbf{x} \rightarrow \mathbf{B}(\mathbf{x})$ specifies the magnetic field and q, \tilde{q} are sections of $T^*\mathcal{M} \otimes T^*\mathcal{M}$ and $T^*\mathcal{N} \otimes T^*\mathcal{N}$, respectively.

- [43] In \hbar units, with our convention, since we have included \hbar in the definition of ω .
- [44] Here, $w_k = -\hbar/2\partial_k \ln n$ is the imaginary component of the complex-valued momentum field introduced in Ref. [31], see Section II.A.

SUPPLEMENTAL MATERIAL

I. DYNAMICAL PATHS

We consider here the total rate of change of the phase of Eq. 8, evaluated along a generic curve γ that connects \mathbf{x}_a to \mathbf{x}_b at initial time and that follows the fluid flow, i.e. $\gamma(t) : [0, 1] \ni s \rightarrow \mathbf{x}(s; t)$ for some convenient parameterization of the curve, $\mathbf{x}(0; t_0) = \mathbf{x}_a$, $\mathbf{x}(1; t_0) = \mathbf{x}_b$ and $\partial\mathbf{x}(s, t)/\partial t = \mathbf{v}(\mathbf{x}(s, t), t)$, where $v^k(\mathbf{x}, t)$ is the velocity field of the probability fluid at time t . We denote this phase $\tilde{\Gamma}[\gamma]$ to emphasize that it is related to a path that is tied to the fluid dynamics, i.e.,

$$\tilde{\Gamma}[\gamma](t) := -\frac{1}{\hbar} \sum_k \int_{\gamma(t)} dx^k \pi_k(t)$$

where $\pi_k(t)$ is the particle momentum field at time t , to be evaluated along γ . The case of a closed curve, $\tilde{\Gamma}_O[\gamma]$, then follows from the results given below upon setting $\mathbf{x}_b(t) = \mathbf{x}_a(t)$, where $\mathbf{x}_a(t)$ ($\mathbf{x}_b(t)$) is the position at time t of a particle that was in \mathbf{x}_a (\mathbf{x}_b) at initial time t_0 . In contrast to the case first addressed in the manuscript (where the path was fixed in time) the rate of change of the line integral involves the *material* derivative of the momentum and contains contributions from the moving path

$$-\hbar \frac{d\tilde{\Gamma}[\gamma]}{dt} = \sum_k \int_{\gamma} dx^k \dot{\pi}_k + \sum_{kj} \int_{\gamma} dx^k \pi_j \partial_k v^j$$

Here, the first term involves the *total* force acting on the fluid elements (Eq. 3)

$$F_k^{\text{tot}} = -\text{Tr}_{\text{el}}(\rho_{\text{el}} \partial_k H_{\text{el}}) - \frac{\hbar^2}{n} \sum_{ij} \xi^{ij} \partial_i (n g_{kj}) - \partial_k Q$$

while for the second term we have

$$\sum_j \pi_j \partial_k v^j = \sum_{ij} \xi^{ij} \pi_j (\partial_k \pi_i) \equiv \partial_k T$$

where $T = \sum_{ij} \xi^{ij} \pi_i \pi_j$ is the classical kinetic energy. As a result,

$$-\hbar \frac{d\tilde{\Gamma}[\gamma]}{dt} = \sum_k \int_{\gamma} dx^k F_k^{\text{tot}} + \Delta T$$

where $\Delta T = T(\mathbf{x}_b(t), t) - T(\mathbf{x}_a(t), t)$. For a closed path the second term disappears and the force entering the first line integral can be simplified to its classical-like contribution

$$F_k = -\text{Tr}_{\text{el}}(\rho_{\text{el}} \partial_k H_{\text{el}}) - \frac{\hbar^2}{n} \sum_{ij} \xi^{ij} \partial_i (n g_{kj})$$

The net result for the rate of change of the phase is thus Eq. 16 of the main text,

$$-\frac{d\tilde{\Gamma}_O[\gamma]}{dt} = \mathfrak{e}^{\text{NBO}} + \mathfrak{e}^{\text{el}}$$

This shows that the magnetic contribution $\mathfrak{E}^{\text{mag}}$ appearing in Eq. 12 is the phase transported along the flow per unit time, i.e. a drift term that only appears when the loop is held fixed in time.

II. TWO-STATE PROBLEM

A. Generalities

In the two-state approximation the electron-nuclear dynamical problem is governed by the Hamiltonian

$$H = \frac{1}{2} \sum_{ij} \xi^{ij} \hat{p}_i \hat{p}_j + H_{\text{el}}(\mathbf{x})$$

where the first term is the nuclear kinetic energy and $H_{\text{el}}(\mathbf{x})$, the electronic Hamiltonian, takes the form

$$H_{\text{el}}(\mathbf{x}) = A(\mathbf{x})\mathbb{I}_2 + \mathbf{B}(\mathbf{x})\boldsymbol{\sigma}$$

in the spinor representation of the wavefunction

$$\Psi(\mathbf{x}) = \begin{pmatrix} \Psi_1(\mathbf{x}) \\ \Psi_2(\mathbf{x}) \end{pmatrix} \in L^2(\mathcal{M}) \otimes \mathbb{C}^2$$

where $\Psi_\sigma(\mathbf{x})$ gives the probability amplitudes of finding the system in the σ^{th} diabatic state. Here, $\mathbf{B}(\mathbf{x}) \in \mathcal{N} \cong \mathbb{R}^3$ is an effective magnetic field for the pseudo-spin describing the local electronic state, whose magnitude B determines the size of the energy gap $E_{\text{gap}}(\mathbf{x}) = 2B(\mathbf{x})$ and whose direction $\mathbf{b}(\mathbf{x})$ specifies the local ‘‘principal axis’’ of the electronic system. Both B and \mathbf{b} can depend on \mathbf{x} , thereby determining complex (adiabatic) energy landscapes, $E_\pm(\mathbf{x}) = A(\mathbf{x}) \pm B(\mathbf{x})$, and non-trivial (i.e., coordinate-dependent) diabatic-to-adiabatic transformations (local rotations of the frame) [40]. Notice that \mathbf{B} affects the geometric properties of the adiabatic bundles while $A(\mathbf{x})$ ‘‘tunes’’ the nuclear dynamics.

In the QHD-EF framework the local electronic state is described by a conditional density matrix, $\rho_{\text{el}}(\mathbf{x}) = \frac{1}{2}(\sigma_0 + \mathbf{s}(\mathbf{x})\boldsymbol{\sigma})$, where $\mathbf{s}(\mathbf{x}) \in \mathcal{N}$ is the polarization vector, with $\|\mathbf{s}\| = 1$ since ρ_{el} describes a pure state. The electronic equation of motion, Eq. 4 with the e - n coupling term given by Eq. 5, can thus be recast as an equation of motion for $\mathbf{s} \equiv \mathbf{s}(\mathbf{x}, t)$. Eq. 4 gives

$$i\hbar\dot{\boldsymbol{\sigma}} = [\mathbf{B}\boldsymbol{\sigma} + \delta H_{\text{en}}, \boldsymbol{\sigma}]$$

where the dot stands for the material derivative and

$$\delta H_{\text{en}} = -\frac{\hbar^2}{4n} \sum_{ij} \xi^{ij} \partial_i (n\mathbf{s}_j \boldsymbol{\sigma})$$

with $\mathbf{s}_j \equiv \partial_j \mathbf{s}$. Here, upon repeated use of the identity $(\mathbf{a}\boldsymbol{\sigma})(\mathbf{b}\boldsymbol{\sigma}) = \mathbf{a}\mathbf{b} + i(\mathbf{a} \times \mathbf{b})\boldsymbol{\sigma}$, we find $[\mathbf{B}\boldsymbol{\sigma}, \boldsymbol{\sigma}] = 2i(\mathbf{B} \times \mathbf{s})\boldsymbol{\sigma}$ and $[\partial_i (n\mathbf{s}_j \boldsymbol{\sigma}), \boldsymbol{\sigma}] = 2i(\partial_i n)(\mathbf{s}_j \times \mathbf{s})\boldsymbol{\sigma} + 2in(\partial_i \mathbf{s}_j \times \mathbf{s})\boldsymbol{\sigma}$, hence

$$\hbar\dot{\boldsymbol{\sigma}} = 2(\mathbf{B} \times \mathbf{s})\boldsymbol{\sigma} - \frac{\hbar^2}{2n} \sum_{ij} \xi^{ij} \{ \partial_i n (\mathbf{s}_j \times \mathbf{s})\boldsymbol{\sigma} + n(\partial_i \mathbf{s}_j \times \mathbf{s})\boldsymbol{\sigma} \}$$

Multiplying by $\boldsymbol{\sigma}$ and tracing over the pseudo-spin degrees of freedom we arrive at the desired equation of motion for \mathbf{s}

$$\begin{aligned} \dot{\mathbf{s}} &= \frac{2}{\hbar} B(\mathbf{b} \times \mathbf{s}) - \frac{\hbar}{2n} \sum_{ij} \xi^{ij} \{ \partial_i n (\mathbf{s}_j \times \mathbf{s}) + n(\partial_i \mathbf{s}_j \times \mathbf{s}) \} \\ &= (\Omega \mathbf{b} + \boldsymbol{\tau}) \times \mathbf{s} - \frac{\hbar}{2} \sum_{ij} \xi^{ij} \partial_i (\mathbf{s}_j \times \mathbf{s}) \end{aligned}$$

which is Eq. 18 of the main text with $\Omega = 2B/\hbar$ and $\boldsymbol{\tau} = -\hbar/2 \sum_{ij} \xi^{ij} \partial_i \ln n \mathbf{s}_j \equiv \sum_{ij} \xi^{ij} w_i \mathbf{s}_j = \sum_j w^j \mathbf{s}_j$. Here, w_k, u^k are the k^{th} components of the ‘‘osmotic’’ momentum and velocity, respectively, defined as the imaginary parts of the complex-valued momentum and velocity fields, $\Pi_k = \hat{\pi}_k \psi / \psi$ and $V^k = \hat{v}^k \psi / \psi$ where ψ is the nuclear wavefunction and $\hat{\pi}_k, \hat{v}^k$ are the Schrödinger-representation mechanical momentum and velocity operators. The equation of motion for \mathbf{s} is purity-conserving, i.e. $\mathbf{s}\dot{\mathbf{s}} = 0$, as must be the case since the original EF electronic equation was for a pure local electronic state.

As for the nuclear dynamics, the Ehrenfest force is readily expressed in terms of the polarization vector

$$F_k^{\text{Eh}} = -\text{Tr}_{\text{el}}(\rho_{\text{el}} \partial_k H_{\text{el}}) = -(\partial_k A + \mathbf{s} \partial_k \mathbf{B})$$

while the *pseudo*-electric contribution requires that the FS (pseudo)metric g_{kj} is expressed in terms of \mathbf{s} . We proceed with calculating the quantum geometric tensor q_{kj} , since this also provides the Berry curvature of the underlying electronic state. This is simple when using Eq. 6, with ρ_{el} given in terms of \mathbf{s} . The result is Eq. 19 of the main text

$$q_{kj} = \frac{1}{4} (\mathbf{s}_k \mathbf{s}_j + i\mathbf{s}(\mathbf{s}_k \times \mathbf{s}_j))$$

which gives the metric (g) and curvature (\mathcal{B}) tensors in the illuminating forms

$$g = \frac{1}{4} d\mathbf{s} d\mathbf{s} \quad \mathcal{B} = -\frac{\hbar}{2} \mathbf{s}(d\mathbf{s} \times d\mathbf{s})$$

where $d\mathbf{s}$ is a three-component 1-form, arranged as a vector of \mathcal{N} . To avoid confusion, their actions on arbitrary tangent vectors $\mathbf{u}, \mathbf{v} \in T_x \mathcal{M}$ read as

$$g(\mathbf{u}, \mathbf{v}) = \frac{1}{4} (\partial_{\mathbf{u}} \mathbf{s})(\partial_{\mathbf{v}} \mathbf{s}) \quad \mathcal{B}(\mathbf{u}, \mathbf{v}) = -\frac{\hbar}{2} \mathbf{s}((\partial_{\mathbf{u}} \mathbf{s}) \times (\partial_{\mathbf{v}} \mathbf{s}))$$

where $\partial_{\mathbf{u}}$ stands for the directional derivative along \mathbf{u} , $\partial_{\mathbf{u}} f = \sum_j u^j \partial_j f$. Here, the vectors $\partial_{\mathbf{u}} \mathbf{s}$ are all tangent to the Bloch sphere $S^2 \subset \mathcal{N}$ swept by the polarization vectors \mathbf{s} (i.e., the projective Hilbert space of the electronic system), since $\mathbf{s}\dot{\mathbf{s}} = 0$ is required by the pure-state nature of the electronic state. Note that g is generally a *pseudo* metric in this context, in particular in this 2-state problem where the state space is the two-dimensional real manifold S^2 , and the $\partial_j \mathbf{s}$'s are necessarily linearly dependent on each other when the number N of nuclear degrees of freedom exceeds two.

The geometric properties of the adiabatic bundles can be obtained from the above expression of the quantum geometric tensor upon setting $\mathbf{s}(\mathbf{x}) = \pm \mathbf{b}(\mathbf{x})$ for the upper and lower energy state, respectively, and depend on the details of the given electronic Hamiltonian, more precisely on the function $\beta : \mathcal{M} \ni \mathbf{x} \rightarrow \mathbf{B}(\mathbf{x}) \in \mathcal{N}$ specifying the magnetic field (i.e. how its orientation varies in nuclear configuration space). However, they can be “pulled back” from those of the spin-problem in a magnetic field, where \mathcal{N} is the parameter space and the cartesian components of the magnetic field form a set of convenient coordinates [14]. In other words, the interesting geometric tensor for our problem, q , is the pull-back of the geometric tensor \tilde{q} (a section of $T^*\mathcal{N} \times T^*\mathcal{N}$) describing the adiabatic dynamics of a spin in a slowly varying magnetic field, i.e., $q_{\mathbf{x}}(\mathbf{u}, \mathbf{v}) = (\beta^* \tilde{q})_{\mathbf{x}}(\mathbf{u}, \mathbf{v}) \equiv \tilde{q}_{\beta(\mathbf{x})}(d\beta_{\mathbf{x}}(\mathbf{u}), d\beta_{\mathbf{x}}(\mathbf{v}))$ for $\mathbf{x} \in \mathcal{M}$ and $\mathbf{u}, \mathbf{v} \in T_{\mathbf{x}}\mathcal{M}$. The components of the metric tensor $\tilde{g} = \Re \tilde{q}$ read (for both the upper and the lower energy state) as

$$\begin{aligned} \tilde{g}_{kj} &= \frac{1}{4} \mathbf{b}_k \mathbf{b}_j = \frac{1}{4B^2} \left(\delta_{kj} - \frac{B_k B_j}{B^2} \right) \\ &= \frac{1}{4B^2} \left(\frac{2}{3} \delta_{kj} - \frac{Q_{kj}}{B^2} \right) \end{aligned}$$

where Q is the traceless tensor defined by $Q_{kj} = 3B_k B_j - \delta_{kj} B^2$. This follows from $\mathbf{b}_k = \partial_k(\mathbf{B}/B) = \frac{1}{B}(\mathbf{e}_k - \frac{B_k}{B} \mathbf{b})$ and gives the required tensor in the form $g = \sum_{k,j} \tilde{g}_{kj} dB^k dB^j$ where $dB^k \equiv \sum_l (\partial_l B^k) dx^l$, for the specific magnetic function β defining the electronic problem. Note that \tilde{g} above is a *pseudo*-metric and reduces to the proper Fubini-Study metric of S^2 when \mathbf{B} is constrained to have a fixed magnitude (as the latter does not affect the spin state). As for the curvature, its components on the canonical basis $dB^k dB^j$ turn out to be

$$\begin{aligned} B_{kj}^{\pm} &= \mp \frac{\hbar}{2B^2} \mathbf{b} \left(\mathbf{e}_k - \frac{B_k}{B} \mathbf{b} \right) \times \left(\mathbf{e}_j - \frac{B_j}{B} \mathbf{b} \right) \\ &\equiv \mp \frac{\hbar}{2B^3} \mathbf{B}(\mathbf{e}_k \times \mathbf{e}_j) \end{aligned}$$

and give the curvature tensor in the form

$$\tilde{\mathcal{B}}_{\pm} = H_x^{\pm} dB^y \wedge dB^z + H_y^{\pm} dB^z \wedge dB^x + H_z^{\pm} dB^x \wedge dB^y$$

where \wedge denotes the wedge product and

$$\mathbf{H}^{\pm} = (H_x^{\pm}, H_y^{\pm}, H_z^{\pm})^t = \mp \frac{\hbar}{2} \frac{\mathbf{B}}{B^3}$$

is the “Berry field” describing a magnetic monopole of charge $q_{\pm} = \mp \hbar/2$ at the origin of \mathcal{N} . The curvature tensor for the given electronic problem is thus obtained from the above expression for $\tilde{\mathcal{B}}_{\pm}$ upon using $dB^i \wedge dB^j = \sum_{kl} J_{kl}^{ij} dx^k \wedge dx^l$, where $J_{kl}^{ij} = \det[\partial(B^i, B^j)/\partial(x^k, x^l)]$ is a Jacobian.

The above results allow one to compute the Berry phase along arbitrary closed paths $\gamma \subset \mathcal{M}$ in parameter space through its mapping to \mathcal{N} space, i.e. by considering the image $\tilde{\gamma} = \beta \circ \gamma$ generated by the magnetic

field function β (the “gap function”). As is well known [14, 41], the Berry phase along a loop $\tilde{\gamma} \subset \mathcal{N}$ is geometric and is given by q_{\pm} times the solid angle subtended by loop. This is the flux of the Berry field \mathbf{H}^{\pm} through an arbitrary surface subtending $\tilde{\gamma}$ (in \hbar units, with our convention). In a typical molecular problem, however, one of the \mathbf{B} components identically vanishes because of time-reversal symmetry, say B_z . Hence, $H_z = 0$, $dB^z \equiv 0$ and \mathcal{B}_{\pm} vanishes identically except at the CI seam. In this case, the image paths $\tilde{\gamma}$ necessarily lie on the xy plane of the \mathcal{N} space and the Berry phase becomes $\mp n\pi$, where n is the winding number of $\tilde{\gamma}$ around the origin of \mathcal{N} .

B. Model problem

For concreteness we consider here a model problem with 3 nuclear degrees of freedom ($\mathcal{M} \cong \mathbb{R}^3$) and a diagonal mass tensor, $\xi^{ij} = \delta^{ij} M^{-1}$. The problem is defined by $\mathbf{B} = Q\boldsymbol{\rho}$ — where $\boldsymbol{\rho}$ is the projection of the position vector on the xy plane and Q a real constant — and exemplifies the situation of a CI seam (the z axis) that presents, as mentioned above, a topological phase. This situation closely resembles the common problem of a spin in an arbitrarily varying magnetic field, except for an important topological difference. The latter problem is indeed defined by $\mathbf{B} = \mathbf{r}$ (henceforth, \mathbf{r} is the position vector in $\mathcal{N} \cong \mathbb{R}^3$) and features an isolated CI point (the origin of \mathbb{R}^3) rather than a CI seam. As a consequence, the parameter manifold for the adiabatic dynamics is simply connected and cannot display any topological phase other than the trivial one, in contrast to the problem considered here where the adiabatic manifold is multiply connected and a topological phase appears naturally when its curvature vanishes.

The nuclear dynamics is also determined by the function $A = A(\mathbf{x})$ that “tunes” the adiabatic potentials and that, depending on its strength, can be used to control the wavepacket dynamics. This function is irrelevant, though, for the geometric properties of interest here and in the numerical applications discussed below will be taken independent of z . This helps reducing the dynamical problem to two nuclear degrees of freedom and two coupled electronic states.

1. Initialization of the dynamics

We are interested in the dynamics of the system when it is initially prepared in an adiabatic state, i.e., when the initial wavefunction takes the form

$$|\Psi_n\rangle = \int_X d\mathbf{x} \psi(\mathbf{x}) |u_n(\mathbf{x})\rangle |\mathbf{x}\rangle \quad (20)$$

where $n = \pm 1$, $|u_n\rangle = \chi_n^1 |1\rangle + \chi_n^2 |2\rangle$, and $\chi_n(\mathbf{x})$ is a (normalized) spinor with definite projection on the local \mathbf{B} axis — i.e., such that $(\mathbf{b}\boldsymbol{\sigma})\chi_{\pm} = \pm \chi_{\pm}$. The latter

represents the adiabatic electronic state in the diabatic basis $\{|1\rangle, |2\rangle\}$.

We begin by addressing certain subtleties inherent in the problem of a spin in a magnetic field, focusing for definiteness on the upper energy state (similar results follow for the lower one). We use the standard parametrization

$$|u_+\rangle = \cos(\theta/2)|1\rangle + e^{i\phi}\sin(\theta/2)|2\rangle \quad (21)$$

for the spin state with +1 projection on the direction $\mathbf{n} = \mathbf{n}(\theta, \phi)$ identified by the polar (θ) and the azimuthal (ϕ) angles of the usual spherical coordinates. As is well known, this parametrization is regular everywhere on S^2 except at the south pole where $|u_+\rangle$ is seen to give $|2\rangle$ with a phase factor that depends on the way the south pole is approached (that is, on the irrelevant angle ϕ). Therefore a second parametrization is required, e.g.,

$$|\tilde{u}_+\rangle = e^{-i\phi}\cos(\theta/2)|1\rangle + \sin(\theta/2)|2\rangle \equiv e^{-i\phi}|u_+\rangle \quad (22)$$

which is related to the previous one by a *gauge* transformation. The *gauge* transformation involved here, however, is *non-standard*: it is a “radical” transformation defined by the function $\varphi(\phi) = \phi$ which increases by 2π after making a turn around the z axis, rather than getting back to its original value. This is a necessary feature of the transformation if $|\tilde{u}_+\rangle$ has to fix the problems of $|u_+\rangle$, since these problems are unaffected by phase transformation functions φ which are smooth all over the manifold (as the ones considered in the main text). These two parametrizations are sufficient to introduce proper frames in the whole adiabatic bundle $\pi: \mathcal{E}_+ \rightarrow S^2$, i.e. the vector bundle based on S^2 whose fibers $\pi^{-1}\{\mathbf{s}\}$ are the + eigenspaces of $\mathbf{s}\sigma$.

Now, since in the spin problem the full set of states (i.e. points of S^2) is required to define a global adiabatic state, a globally smooth electronic state (hence a globally smooth nuclear wavefunction) *cannot* be introduced. Rather, in the adiabatic wavefunction for the total system one has to use a pair $\{|\psi_0\rangle, |u_+\rangle\}$ for \mathbf{r} such that $\mathbf{b}(\mathbf{r}) \neq -\mathbf{e}_3$ and a second pair $\{|\tilde{\psi}_0\rangle, |\tilde{u}_+\rangle\}$ for $\mathbf{b}(\mathbf{r}) \neq +\mathbf{e}_3$, with $\tilde{\psi}_0 = \psi_0 e^{i\phi}$ in overlapping regions. Here, $\psi_0(\mathbf{r})$ and $\tilde{\psi}_0(\mathbf{r})$ are nuclear wavefunctions representing the same state in the two different *gauges* defined above and the \mathbf{e}_k 's are canonical orthonormal vectors in $\mathcal{N} \cong \mathbb{R}^3$. In this problem the field direction is also the direction of the position vector, $\mathbf{b} \equiv \hat{\mathbf{r}}$, and the spherical coordinates (θ, ϕ) become the spherical angles of the nuclear position vector \mathbf{r} . Hence, one can use $\psi_0(\mathbf{r})$ and $|u_+(\hat{\mathbf{r}})\rangle$ for the whole space except a small cone around the negative z axis, or the pair $\tilde{\psi}_0(\mathbf{r})$ and $|\tilde{u}_+(\hat{\mathbf{r}})\rangle$ everywhere except a small cone around the positive real axis. In other words, $\tilde{\psi}(\mathbf{r}) = e^{i\phi}\psi(\mathbf{r})$ holds everywhere except along z , where ϕ would be undefined in any case.

The vector potentials corresponding to the above *gauge* choices can be computed with a direct calculation and turn out to be, respectively,

$$\mathbf{A} = -\frac{1}{2}\frac{\tan(\theta/2)}{r}\mathbf{e}_\phi \quad \tilde{\mathbf{A}} = -\frac{1}{2}\frac{\cot(\theta/2)}{r}\mathbf{e}_\phi$$

where \mathbf{e}_ϕ is the unit vector along ϕ . They clearly present a singularity, respectively, for $\theta = \pi$ and $\theta = 0$ (the Dirac strings), but both describe the same Berry field where they apply, i.e. $\hbar\nabla \times \mathbf{A} = \hbar\nabla \times \tilde{\mathbf{A}} = \mathbf{H}^+$. When the underlying electronic states are paired with suitable nuclear wavefunctions, these vector potentials determine the mechanical momentum and velocity fields, and fix their circulation, *modulo an appropriate “quantum”*. In a sense they fix the symmetry of the momentum and velocity fields and their vortex structure. Notice though that there is nothing special about the z axis. Suitable *gauge* transformations exist that reorient the z axis and the ensuing electronic frame can be used to align the symmetry axis of the nuclear velocity field (and its half vortex-line) along *arbitrary* directions.

For definiteness we choose the first *gauge* and first set ψ to be real. The momentum field then reads as

$$\boldsymbol{\pi} = +\frac{\hbar}{2}\frac{\tan(\theta/2)}{r}\mathbf{e}_\phi$$

everywhere except on the negative z axis (and where ψ_0 eventually vanishes). Like \mathbf{A} , this field has a singularity on the negative z axis and this cannot be removed by changing the *gauge* with a regular transformation, since $\boldsymbol{\pi}$ is *gauge* invariant and the above expression holds for arbitrarily small cones around the negative z axis, i.e. it cannot be remedied with any choice of $\tilde{\psi}_0$ on the z axis. And choosing ψ_0 with a node on the negative z axis removes the problem of using a pair of *gauges* (since $|u_+\rangle$ for $\theta = \pi$ is then useless) but does not remove the singularity in the momentum and velocity fields. The circulation of this momentum field along a circular path at constant latitude (as defined by Eq. 8) gives the well-known adiabatic result

$$\Gamma_O(\theta) = -\frac{1}{2}\int_0^{2\pi}\frac{\tan(\theta/2)}{r}r\sin(\theta)d\phi = -2\pi\sin^2\left(\frac{\theta}{2}\right)$$

which represents the flux of the Berry field on the sphere portion which is above θ . For θ tending to π , i.e. when the loop shrinks to a point on the *negative* z axis, this tends to -2π , which is yet zero but only mod 2π . This amounts to a non-vanishing first Chern number, here of value -1, that reflects the non-trivial topology of \mathcal{E}_+ and that manifests itself in a vortex structure of the momentum field of the + adiabatic state on the negative z axis, with the above *gauge* choice. Replacing $\psi_0(\mathbf{r})$ with an arbitrary but smooth function changes the momentum field locally but not its circulation, hence the same result holds for *arbitrary* nuclear wavefunctions. In this sense, the *gauge* choice determines the symmetry of the momentum field and its vortex structure, modulo a longitudinal vector contribution ($\hbar\nabla\mathfrak{I}\ln\psi_0$). Clearly, upon using $|\tilde{u}_+\rangle$ one defines a different class of states, with a different circulation around that axis. The difference as compared with the previous case is 2π and now a vortex structure appears on the positive z axis. And, as mentioned above, with an appropriate rotation one can

make the half-line vortex pointing in arbitrary directions. Actually, this half-line vortex is not even a necessary feature of the adiabatic state: the implicit assumption above was that $\boldsymbol{\pi}$ was well-defined wherever \mathbf{A} was not singular, i.e., that ψ_0 did not vanish somewhere (otherwise a singularity would also arise from the canonical momentum contribution, $\hbar\nabla\Im\ln\psi_0$). If $\psi_0(\mathbf{r})$ has zeros one can exploit their presence to smoothly (but radically) change the underlying *gauge*. For instance, if $\psi_0(\mathbf{r}) \equiv 0$ in the xy plane one can smoothly switch from $|u_+\rangle$ to $|\tilde{u}_+\rangle$ and thus remove the half-line vortex. The price to be paid is that now the singularity in the momentum field extends to the xy plane. In this case, the circulation $\Gamma_O(\theta)$ for the loops at constant latitude considered above suddenly jumps from $-\pi$ to π when $\theta = \pi/2$ and tends to zero for both $\theta \rightarrow 0$ and $\theta \rightarrow \pi$, being completely undefined for $\theta = \pi/2$.

The above ‘‘frustration’’ problems do not arise in our model molecular problem, where the adiabatic state involves only the points at the equator of S^2 . In this case a single parametrization suffices, e.g.

$$|u_+\rangle = \frac{1}{\sqrt{2}}(|1\rangle + e^{i\phi}|2\rangle) \quad (23)$$

whose corresponding Berry vector potential reads as

$$\mathbf{A} = -\frac{1}{2\rho}\mathbf{e}_\phi$$

Here, ϕ can be identified with the azimuthal angle of the position vector and ρ is the distance from the z axis. As anticipated above, the Berry field vanishes everywhere except on the z axis (i.e., $\nabla \times \mathbf{A} \equiv \mathbf{0}$ where \mathbf{A} is well defined), however, the circulation of \mathbf{A} around that axis is non-vanishing and describes a topological phase. The latter can be obtained by considering a circular path of radius ρ (since this value is the same for any homotopic loop thanks to $\nabla \times \mathbf{A} = \mathbf{0}$), and it is easily seen to be non-trivial,

$$\oint \mathbf{A}d\mathbf{x} = -\int_0^{2\pi} \frac{1}{2\rho}\rho d\phi = -\pi$$

This is also the value (modulo 2π) of the circulation of the momentum field according to Eq. 8, with the above *gauge* choice of the electronic wavefunction. Indeed, arguing as above, if we take ψ_0 real and use the above *gauge* we have $\boldsymbol{\pi} = \frac{\hbar}{2\rho}\mathbf{e}_\phi$, which gives $-\pi$ when Eq. 8 is evaluated along a loop encircling the z axis once. And the same value of the phase results when replacing $\psi_0(\mathbf{x})$ with an arbitrary smooth function, not vanishing in extended regions. A radically different *gauge* choice, e.g.,

$$|\tilde{u}_+\rangle = \frac{1}{\sqrt{2}}(e^{-i\phi}|1\rangle + |2\rangle)$$

gives a different circulation ($+\pi$) when paired with smooth nuclear wavefunctions. And, as above, one can even interpolate between the two situations by selecting

ψ_0 with a node in the xy plane and switching between the two *gauges* when going from $z > 0$ to $z < 0$.

In other words, when selecting an *adiabatic* state, the circulation of the momentum field (according to Eq. 8) is ‘‘pinned’’, by construction, to the adiabatic value, but variations of $2\pi n$ are possible depending on the singularities of $\boldsymbol{\pi}$ due to either \mathbf{A} (through its topological frustration) or ψ (through its nodal structure).

2. Phase dynamics

We now address the behavior of the phase defined by Eq. 8, when the dynamics is started from an adiabatic state. The electron dynamics is described by the equation of motion of the polarization vector which, as seen above, reads as

$$\dot{\mathbf{s}} = (\Omega\mathbf{b} + \boldsymbol{\tau}) \times \mathbf{s} - \frac{\hbar}{2M} \sum_j (\partial_j \mathbf{s}_j) \times \mathbf{s}$$

and the rate of phase change appearing on the r.h.s. of Eq. 12 can be expressed as

$$-\frac{d\Gamma_O[\gamma]}{dt} = \sum_X \oint_\gamma \Phi^X \quad X=\text{NBO,el and mag}$$

where Φ^X are the following 1-forms,

$$\Phi^{\text{NBO}} = \hbar^{-1}\mathbf{B}ds \quad (24)$$

$$\Phi^{\text{el}} = \frac{1}{2}\boldsymbol{\tau}ds - \frac{\hbar}{4M} \sum_j \partial_j \mathbf{s}_j ds \quad (25)$$

and

$$\Phi^{\text{mag}} = +\frac{1}{2}(\boldsymbol{\nu} \times \mathbf{s})ds \quad (26)$$

Here, $\Omega = 2B/\hbar$ is the ‘‘intrinsic’’ precession frequency, $\boldsymbol{\tau} = \frac{1}{M} \sum_j w_j \mathbf{s}_j$ is the ‘‘nuclear torque’’ and $\boldsymbol{\nu} = \frac{1}{M} \sum_j \pi_j \mathbf{s}_j$ is the ‘‘drift velocity’’, π_k and w_k being, as usual, the real and imaginary parts of the complex-valued field $\Pi_k = -i\hbar\partial_k \ln\psi - \hbar A_k$. The advantage of this formulation is that now the circulations $\mathbf{e}^X = \oint_\gamma \Phi^X$ are mapped onto the Bloch sphere S^2 : for \mathbf{x} moving along a curve γ , $\mathbf{s}(\mathbf{x}) \in S^2$ traces a curve $\tilde{\gamma}$ on the sphere, $\boldsymbol{\tau}, \boldsymbol{\nu}$ and ds are tangent to the sphere, while \mathbf{B} can have both tangent and normal components, depending on the real-space position \mathbf{r} . This gives immediately a simple way to express the geometric phase and its rate of change at any time, once the polarization field \mathbf{s} is known.

To see this, consider the ‘‘northern’’ *gauge* in the \mathcal{N} space where the Bloch sphere can be embedded, i.e., $|u_+\rangle$ of Eq. 21. The corresponding vector potential $\mathbf{A} = -\tan(\theta/2)\mathbf{e}_\phi/2r$ can be written in terms of \mathbf{s} by noticing that

$$\tan(\theta/2) = \sqrt{\frac{1 - \cos\theta}{1 + \cos\theta}} = \sqrt{\frac{1 - s_z}{1 + s_z}}$$

and

$$\mathbf{e}_\phi = -\frac{s_y}{\sqrt{s_x^2 + s_y^2}}\mathbf{e}_1 + \frac{s_x}{\sqrt{s_x^2 + s_y^2}}\mathbf{e}_2$$

where s_x, s_y and s_z are the cartesian components of \mathbf{s} . The dependence of \mathbf{A} on \mathbf{s} is specific of this *gauge* choice (since \mathbf{A} is *gauge* dependent while \mathbf{s} is not) but the circulation of \mathbf{A} is the same for any *gauge* choice (everywhere on \mathcal{S}^2 except at the south pole where \mathbf{A} is ill-defined). Therefore, for a curve γ that is mapped onto the curve $\tilde{\gamma}$ on the sphere, the equation

$$\oint_{\tilde{\gamma}} \mathbf{A} ds = -\frac{1}{2} \oint_{\tilde{\gamma}} \sqrt{\frac{1-s_z}{1+s_z}} \frac{(\mathbf{e}_3 \times \mathbf{s})}{\sqrt{s_x^2 + s_y^2}} ds \quad (27)$$

provides a convenient expression for the geometric phase in terms of \mathbf{s} only. This expression is valid for arbitrary curves, provided their images $\tilde{\gamma}$ do not pass through the south pole. This limitation can be easily overcome, however, since the position of the south pole is arbitrary and can be changed with a rotation of the coordinate system, i.e. one can always pick a point of \mathcal{S}^2 not belonging to $\tilde{\gamma}$ and use it to orient the south pole when computing the phase using Eq. 27.

Eq. 27 and Eqs. 24, 25 and 26 allow one to extract the key dynamical information from an exact wavepacket dynamics, without resorting to the exact factorization of the wavefunction. Specifically, at any time, given the spinor field $\Psi_\sigma(\mathbf{x})$ representing the two-state *e-n* wavefunction in the electronic diabatic basis $\{|1\rangle, |2\rangle\}$, the polarization field can be written as $\mathbf{s}(\mathbf{x}) = \mathbf{\Sigma}(\mathbf{x})/n(\mathbf{x})$ where $n(\mathbf{x}) = \Psi^\dagger(\mathbf{x})\Psi(\mathbf{x}) \equiv \sum_\sigma |\Psi_\sigma(\mathbf{x})|^2$ is the nuclear density and $\mathbf{\Sigma}(\mathbf{x}) = \Psi^\dagger(\mathbf{x})\boldsymbol{\sigma}\Psi(\mathbf{x})$ or, explicitly,

$$\begin{aligned} \mathbf{\Sigma}(\mathbf{x}) &= 2\Re(\Psi_1^*(\mathbf{x})\Psi_2(\mathbf{x}))\mathbf{e}_1 + \\ & 2\Im(\Psi_1^*(\mathbf{x})\Psi_2(\mathbf{x}))\mathbf{e}_2 + \\ & (|\Psi_1(\mathbf{x})|^2 - |\Psi_2(\mathbf{x})|^2)\mathbf{e}_3 \end{aligned}$$

The field \mathbf{s} describes the local electronic states and can be used to compute the geometric phase along arbitrary paths $\gamma : u \rightarrow \mathbf{x}(u)$, through their images $\tilde{\gamma} : u \rightarrow \mathbf{s}(\mathbf{x}(u))$, as well as the non-conservative fields \mathbf{f}^X generating the electromotive forces of Eqs. 24, 25 and 26 (i.e. through $\Phi^X = \mathbf{f}^X ds$). The latter can be recast as

$$\mathbf{f}^{\text{NBO}} = \hbar^{-1} \mathbf{B} \quad (28)$$

$$\mathbf{f}^{\text{el}} = -\frac{1}{2Mn} \sum_j \left(w_j \partial_j \mathbf{\Sigma} + \frac{\hbar}{2} \partial_j^2 \mathbf{\Sigma} \right) \quad (29)$$

$$\mathbf{f}^{\text{mag}} = -\frac{1}{2Mn} \left(\mathbf{s} \times \sum_j \pi_j \partial_j \mathbf{\Sigma} \right) \quad (30)$$

(upon removing some terms that do not contribute to their circulations) and require the first and second spatial derivatives of the vector $\mathbf{\Sigma}(\mathbf{x})$, along with the momentum fields π_j and w_j . These latter fields are the real

and imaginary parts, respectively, of the complex-valued momentum

$$\Pi_j(\mathbf{x}) = \frac{\Psi^\dagger(\mathbf{x}) \hat{p}_j \Psi(\mathbf{x})}{\Psi^\dagger(\mathbf{x}) \Psi(\mathbf{x})} \quad (31)$$

which, written in this way, requires just the canonical momentum, with no reference to any phase choice for the local electronic wavefunction [Note that $\Psi(\mathbf{x})$ and \hat{p}_j are *gauge* invariant for the full *e-n* problem, and that \hat{p}_j gives the mechanical momentum when averaged over the electronic state, $\hat{\pi}_j = \langle \hat{p}_j \rangle_{\text{el}}$].

Note that Eq. 31 could be also used to compute directly the geometric phase with the help of Eq. 8, with results equivalent to those obtained from Eq. 27. However, this approach does not give full access to the electronic properties, specifically the electromotive forces and the fields of Eqs. 28, 29 and 30 generating them. Furthermore, the polarization vector is also useful to compute the local adiabatic populations $p_\pm(\mathbf{x}) = (1 + \mathbf{s}_\pm \cdot \mathbf{s})/2$ (where \mathbf{s}_\pm are the polarization for the \pm adiabatic states, i.e. $\mathbf{s}_\pm = \pm \hat{\mathbf{r}}$), from which the adiabatic populations follow as

$$P_\pm = \int d\mathbf{x} n(\mathbf{x}) \frac{1 + \mathbf{s}_\pm \cdot \mathbf{s}}{2}$$

C. Numerical applications

As mentioned above, in the numerical application we focused on a 2-state 2-dimensional problem by selecting the scalar $A(\mathbf{x})$ to be a function of x, y only. We set

$$A(\mathbf{x}) = \frac{1}{2} M \omega_x^2 x^2 + \frac{1}{2} M \omega_y^2 y^2$$

with parameters typical of a molecular problem (the system mass $M = 1$ u.m.a. and $\omega_x = \omega_y = \omega = 4.5563359 \times 10^{-3}$ a.u., corresponding to 1000 cm^{-1}), while for the effective magnetic field we used a linear-vibronic coupling form

$$\mathbf{B} = \kappa_x x \mathbf{e}_1 + \kappa_y y \mathbf{e}_2$$

with $\kappa_x = \kappa_y = \kappa = 0.1$ a.u.. The problem represents thus a linear $E \otimes e$ Jahn-Teller model, with adiabatic states $E_\pm(\mathbf{x}) = \frac{1}{2} M \omega^2 \rho^2 \pm \kappa \rho$.

We solved the time-dependent Schrödinger equation (TDSE) using a standard Split-Operator (SO) algorithm in conjunction with Fast-Fourier-Transforms (FFTs) to go back and forth between real- and momentum-space. The wavefunction was represented on a fine grid (1024×1024) centered at the CI point at $\mathbf{x} = \mathbf{0}$ and of length $20 a_0$ along each direction. A small time step of $\Delta t = 0.1$ a.u. was adopted to ensure a good sampling of the geometric phase over time and an accurate solution of the TDSE. We considered two initial wavefunctions, obtained by combining a “nuclear” wavepacket ($\psi_0(\mathbf{x})$) with two (slightly) different electronic states ($\chi_\sigma(\mathbf{x})$), i.e.

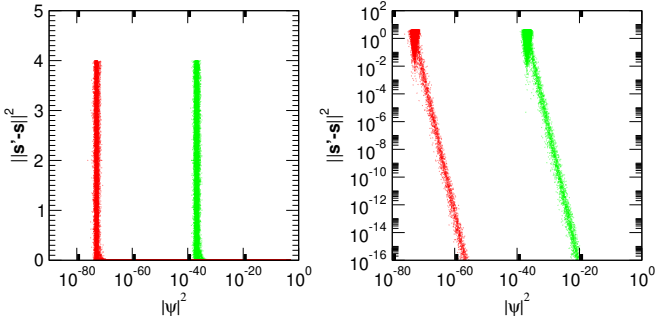


Figure 2. Squared error intrinsic in FFT arithmetics when computing the polarization field $\mathbf{s}(\mathbf{x})$, as a function of the nuclear density at the grid points (see text for details). Green and red symbols for double and quadruple precision arithmetics, respectively.

$\Psi_\sigma(\mathbf{x}) = \psi_0(\mathbf{x})\chi_\sigma(\mathbf{x})$. The nuclear wavepacket $\psi_0(\mathbf{x})$ was a Gaussian centered at $x_0 = -2\kappa/M\omega^2$ and $y_0 = 0$, with ground-state width along both x and y ($\Delta x = \Delta y = \sqrt{\hbar/2m\omega}$) and zero nominal momentum along both directions. As for the electronic state, on the other hand, we considered both the true adiabatic ground-state of Eq. 20 with the *gauge* $\chi = [-e^{-i\phi}, 1]^t/\sqrt{2}$ (where ϕ is, as usual, the azimuthal angle of the position vector \mathbf{x}) and the uniform state defined by the electronic ground state at the center of the initial nuclear wavepacket. In other words, we choose $|u(\mathbf{x})\rangle = \frac{1}{\sqrt{2}}(-e^{-i\phi}|1\rangle + |2\rangle)$ in the first, “correlated” case and $|u(\mathbf{x})\rangle \equiv |u_-(x_0, y_0)\rangle$ in the second, “uncorrelated” case. The latter is a popular (pragmatical) representation of the electronic ground-state, but it does not correspond to a true adiabatic state. The difference between the two is globally minimal (if the wavepacket is narrow enough) but evident: the first is current-carrying even if the nuclear wavepacket is chosen real as described above (it presents a non-vanishing velocity directed along the negative ϕ direction, although very small with the chosen parameters), the second presents a non-vanishing population on the excited state and has a vanishing velocity field. Importantly, the first displays a non-trivial, topological Berry phase ($+\pi$) for any loop encircling once the origin, inherited from the adiabatic connection, while the second has a trivial connection.

We computed the geometric phase along selected paths at each time-step, using the discretized version of Eq. 27, namely

$$\Gamma_O = -\frac{1}{2} \sum_{i=1}^{N_\gamma} \sqrt{\frac{1-s_z(\mathbf{x}_i)}{1+s_z(\mathbf{x}_i)}} \frac{(\mathbf{e}_3 \times \mathbf{s}(\mathbf{x}_i))}{\sqrt{s_x^2(\mathbf{x}_i) + s_y^2(\mathbf{x}_i)}} \Delta \mathbf{s}_i$$

where the \mathbf{x}_i 's are the N_γ points on the real-space grid that are used to represent the desired path γ , $\mathbf{s}(\mathbf{x})$ is the instantaneous polarization field and $\Delta \mathbf{s}_i = (\mathbf{s}(\mathbf{x}_{i+1}) - \mathbf{s}(\mathbf{x}_{i-1}))/2$ (with $\mathbf{x}_{N_\gamma+1} = \mathbf{x}_1$ and $\mathbf{x}_{N_\gamma} = \mathbf{x}_0$ for a closed path). The chosen paths are circles centered at the origin with different radii, encompassing the inner and the outer classical turning points of the ground-state valley.

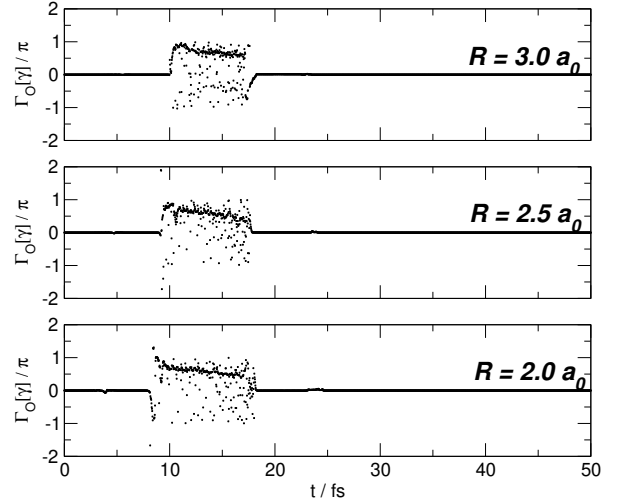


Figure 3. Estimated error in the computed geometric phase. Difference between results obtained in double precision arithmetics and $\epsilon_{\text{th}} = 10^{-20}$, and results obtained in quadruple precision arithmetics and $\epsilon_{\text{th}} = 10^{-30}$.

Calculation of polarization field $\mathbf{s}(\mathbf{x})$ was critical at the beginning of the dynamics, when the nuclear density is small on a large portion of the grid and conflicts with the accuracy of the numerical implementation, in particular the arithmetics underlying the FFTs. This can be easily checked with a fake propagation step using $\Delta t = 0$ – which only involves a forward and a backward Fourier transformation – by comparing the polarization field $\mathbf{s}'(\mathbf{x})$ computed after the transformation with that prior to the transformation ($\mathbf{s}(\mathbf{x})$). The results of such test are shown in Fig. 2, which reports the squared error $\|\mathbf{s}' - \mathbf{s}\|^2$ at \mathbf{x} as a function of the nuclear density $n(\mathbf{x})$, for the true adiabatic state defined by Eq. 20. This problem has no physical implications for the geometric phase since this phase has no physical meaning when the probe path lies entirely or partially in a region of small nuclear density (i.e., where the system has little probability to be found). Nevertheless, in order to alleviate it, we decided to update the polarization field only at those grid points where the nuclear density was larger than a numerically reasonable threshold ϵ_{th} , and used quadruple precision to set this threshold to 10^{-30} (Fig. 2). To this end we relied on the Fortran 2003 interface to the FFTW support for the nonstandard `_float128` quadruple-precision type provided by `gcc` (<http://www.fftw.org/>). The results show a marginal difference only from those obtained using double precision arithmetics and a threshold of 10^{-20} : as seen in Fig. 3 the main differences arise for $t \lesssim 20$ fs, that is, when the wavepacket has yet a tiny weight on the initially unoccupied portion of the valley (which is accounted differently with the two thresholds mentioned above). At longer times, precision does not affect anymore the phase value.

The evolution of the geometric phase for the correlated initial state are discussed in the main text, see Fig. 1.

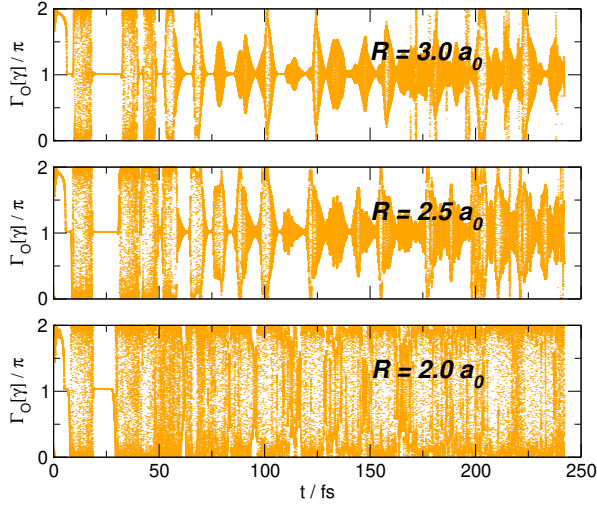


Figure 4. Same as in Fig. 1(e) but for an uncorrelated initial state approximating the true ground adiabatic state.

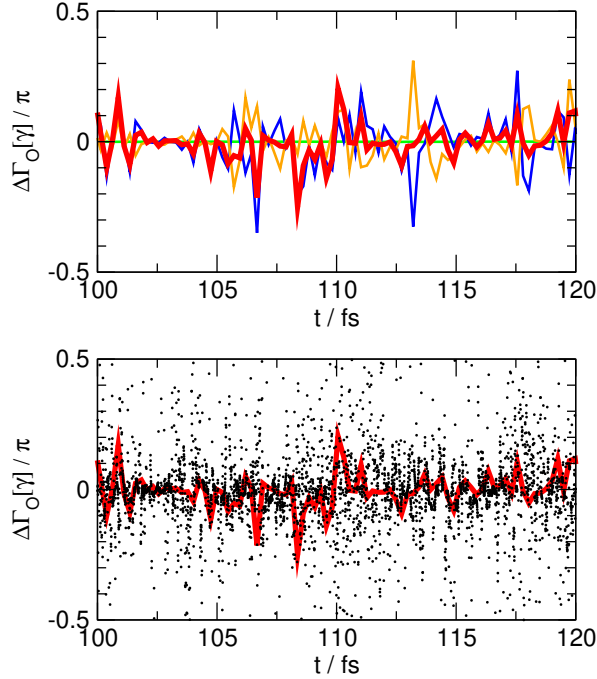


Figure 5. Decomposition of the dynamically-induced geometric phase change in terms of its contributing components. $\Delta\Gamma_O[\gamma]$ is the phase difference accumulated in a time step of $\Delta t = 1$ a.u., for a circle of radius $R = 1 a_0$ centered at the CI point, and an initial correlated ground-state. Bottom panel: the (minus) total electromotive force (red) is compared with the difference $\Gamma_O[\gamma](t) - \Gamma_O[\gamma](t - \Delta t)$ in the phase computed at neighboring times (dots). Top panel: the same total electromotive force of the bottom panel is reported along with the NBO (green), *pseudo-electric* (blue) and *pseudo-magnetic* (orange) components.

The uncorrelated initial state gives rise to qualitatively similar results but presents a more marked non-adiabatic behaviour (see Fig. 4), in accordance with an excited probability which is two order of magnitude larger than in the previous case, $P_+ \approx 10^{-3}$. Noteworthy, despite the evident variations the phase oscillates around the adiabatic value π and gets back to this value at regular time intervals.

Finally, we further computed the total electromotive force and their contributing non-Born-Oppenheimer, *pseudo-electric* and *pseudo-magnetic* components. The results are shown in Fig. 5 for a circle of small radius, $R = 1.0 a_0$, where these forces are more evident, for the correlated initial state. The electromotive force and its contributing components were obtained from Eqs. 28, 29 and 30, at intervals much larger than the time step used for the dynamics in order to reduce the computational cost (Eqs. 28-30 require the first and second spatial derivatives of \mathbf{s} , hence add FFT calls to the propagation). As seen from that figure, the NBO component contributes little to the phase change, while the *pseudo-electric* one plays the major role. This implies that these dynamically-induced phase changes cannot be captured by approximate methods like Ehrenfest dynamics which only account for the NBO term.